

Mimicry of Fish Swimming Patterns in a Robotic Fish

Jian-Xin Xu, Qinyuan Ren, Wenchao Gao and Xue-Lei Niu
Department of Electrical and Computer Engineering
National University of Singapore, Singapore 117576
Email: elerq@nus.edu.sg

Abstract—This paper¹, presents a novel approach for realizing Carangiform fish swimming patterns by a robotic fish. A video recording system is first set up to capture real fish behaviors. From robotic perspective, three basic Carangiform fish swimming patterns, “cruise”, “cruise in turning”, and “C sharp turning”, are extracted. Base on observations, the mapping between the fish action parts (angular displacements) and the fish swimming patterns are formulated. Hence, the three swimming motion patterns are implemented on a multi-joint robotic fish. Finally, the effectiveness of the approach is verified through experiment results.

I. INTRODUCTION

The astonishing swimming abilities of fish have inspired many researchers to develop a new kind of underwater robots whose structures are intimated from the fish morphology. As the first step of designing and controlling a fish-like robot, it is necessary to find out how fishes swim. In nature, most fishes generate thrust principally via body and/or caudal fin, namely BCF swimmers [1]. According to undulatory motion versus oscillatory motion, BCF swimming modes can be classified mainly into three categories: Anguilliform, Carangiform, and Thunniform [1][2]. In this paper, we only focus on Carangiform types of fish, since their movement is one of the easiest to replicate from the mechanical design perspective. As pointed out in [3], all Carangiform fish movements can be classified into several basic fish swimming motion patterns, such as “cruise”, “cruise in turning”, and “C sharp turning”. Since it is difficult to formulate the explicit hydrodynamics and kinematics of various swimming patterns, modeling fish behaviors and generating fish-like motion patterns in robotic fishes have become one of the hot topics in current research.

The approaches that have been adopted for modeling and generating robotic fish locomotion are based on dynamic models, kinematic models, or central pattern generator (CPG). The dynamics-based approach employs hydrodynamic models for swimming motion generation. In [4][5], a planar model is proposed for the Carangiform swimming based on a reduced Euler-Lagrange function. The model describes the interaction between the rigid body and the surrounding fluid. Based on the planar model, non-linear control methods are developed for locomotion generation. However, complex fish maneuvers

are not easy to produce through hydrodynamic analysis. When fishes swim, the mechanisms of the interaction between fish bodies and fluid are complex. Kinematics-based approach tries to find out fish body kinematic models in various fish swimming patterns. Several interpreted body kinematic models with special motion patterns are build up. For instance, a traveling wave function is adopted to model cruise motion kinematics [6], and a kinematic model of C sharp turning is presented in [7]. CPG is utilized to generate rhythmic movements for each actuator of the robotic fish. In [8], a CPG network with non-linear oscillators is established and investigated for gait generation of robotic fish. In [9], an amphibious robot, which can make fish-like locomotion underwater by using CPG, is developed. These works show that CPG-based approaches are easy to design, quick to implement, and able of online adjustment. Due to the rhythmic feature of CPG, CPG-based approach is easy to generate cruise swimming pattern. Nevertheless, how to apply CPG to generate maneuvering swimming patterns is still under research.

In this paper, we propose a novel approach for realizing basic Carangiform fish swimming patterns by a multi-joint robot. Real fish behaviors are captured from a video recording system, and three basic swimming patterns, “cruise”, “cruise in turning”, and “C sharp turning”, are extracted. From robotic perspective, fish swimming patterns can be represented by a set of fish actuation movements. In this work, based on observations, these movements are modeled and implement on a robotic fish to generate fish-like swimming patterns.

The paper is organized as follows. Section II presents the multi-joint robotic fish model and the schematic structure of a robotic fish. In Section III, study from a real carp swimming based on a video recording system is described, and three basic fish swimming patterns are extracted and modeled, namely, “cruise”, “cruise in turning”, and “C sharp in turning”. In Section IV, real robotic fish experiments are given to show the effectiveness of the proposed approach. Finally, Section V gives the conclusion.

II. DESIGN OF ROBOTIC FISH

A. A multi-joint robotic fish model

In Carangiform swimming, the front two-thirds of the fish’s body moves in a largely rigid way, with the propulsive being confined to the rear third of the fish’s body. The tail is

¹This work was supported by the STARFISH project of Defence Science and Technology Agency (DSTA), Singapore, under Grant R-263-000-622-232

connected to the body by a penduncle that is a slender region with generally negligible hydrodynamic influence.

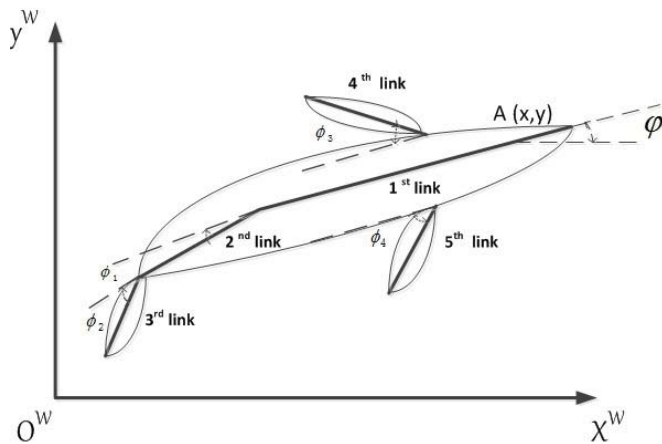


Fig. 1. Multi-joint robotic fish model.

As shown in Fig.1, Carangiform fish can be modeled as a multi-joint model. The main body of the fish is idealized as two rigid parts connecting together. The tail and the fins can be interpreted as rigid lifting surfaces, generating thrust through flapping and heaving motions in accordance with hydrodynamic principles. $X^w O^w Y^w$ is the world coordinates system. The position and orientation of whole body are described by three coordinates, x^w , y^w , and ψ . x^w and y^w denote the position of the point A in the one-eighth of body length (as the midpoint between two eyes of carps), while ψ denotes the angle from $+x^w$ -axis to the 1st link. The movement of whole fish body in the world coordinate system is described as $f_m(x^w, y^w, \psi, t)$. ϕ_i ($i = 1, 2, 3, 4$) denote the actual control angles, which are joint angles between neighboring links.

Robotic fish swimming patterns can be generated by controlling the motion of body. The thrust of the robotic fish swimming is generated from its body bending, fins heaving and tail flapping. Hence, the motion of the robotic fish is controlled by the directly actuated “shape” through manipulating $\phi_i(t)$. Thus, there exists a relationship or a mapping between the joint angular displacement $\phi_i(t)$ and individual swimming patterns. In this paper, we explore this mapping through observations on a real fish swimming, which is described by subsequent sections.

B. Schematic structure of the robotic fish

According to the multi-joint robotic fish model, we have developed a robotic fish. Fig.2 shows its schematic structure. The robotic fish is approximately 25cm long. It consists of four servo motors, a micro processor, a wireless communication module, five aluminum links, a set of sensors, and several other peripherals. As shown in Fig.3, two motors fixed on both sides of the fish head are utilized to control the pectoral fins. The other two motors that control the movements of the fish body segments and the tail are concatenated together to act as two joints. A micro processor is responsible for processing

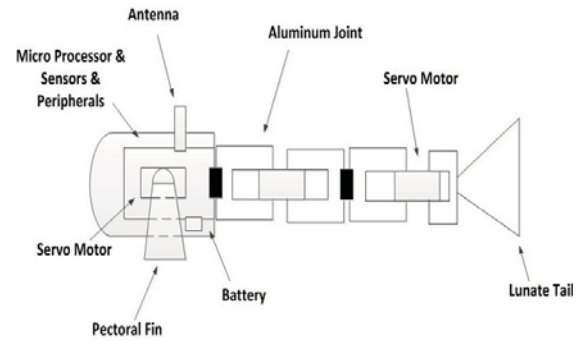


Fig. 2. Structure of the robotic fish.

sensor data, transferring diagnostic information via a blue tooth wireless link, making decisions and controlling servo motors. A set of sensors, including a digital compass, a three-axis gyro and three accelerate meters, are utilized to estimate the motion state of the robotic fish.

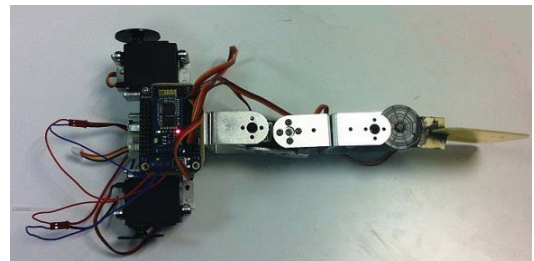


Fig. 3. Framework of the robotic fish without water proof skin covered.

III. STUDY OF CARPS SWIMMING

A. Description the video recording system

Video recording systems and image analysis theories have been widely applied in fish biological properties or swimming hydrodynamics analysis, but are seldom used for robotic fish motion analysis and control. In order to collect sufficient fish motion information for the purpose of exploring fish swimming patterns, a video recording system is developed, as shown in Fig. 4. Carps are chosen as the observation objects, since they are the typical Carangiform fishes. One carp with a length of 19cm is video-taped during swimming in a fish tank, which is 70cm × 30cm × 40cm.

Data are collected by video-taping the motion of the fish at 60 frames per second using a high speed and resolution video system. The video system consists of three cameras and a processing computer. To facilitate camera calibration and fish motion estimation, a special pattern is attached to three sides of the tank. As shown in Fig.5, each square in the pattern is 28mm × 28mm.

The movements of the carp actuation parts are extracted from image process. Though the 3D imaging is available for the fish locomotion analysis, based on the multi-joint robotic fish model given in Section II, only 2D plane (overhead view) images are used. Generally, in order to receive accurate motion



Fig. 4. The video recording system. Three cameras are used simultaneously to record three views, lateral, posterior and overhead. The overhead view is obtained by the high-speed camera, the resolution of every captured image reaches 1920×1080 pixels, and the other two views are obtained by two web cameras.

estimation parameters based on image process, camera should be calibrated. Since the camera lens we used are complicated and the refraction effect from water cannot be ignored, the traditional pin hole model or simple distortion model would not be suited for calibrating the camera. To solve this problem, a special pattern is used. As shown in Fig.5, at the current position of the fish, we construct a image coordinate system UOV . In each image, the shape of the fish is confined to 4×7 grids. Within this area, the distance between any two points can be described as:

$$|D| = |m(u, v) - n(u, v)| \times (T/|\overline{ON}|)$$

where m, n are any two pixels in the image, the point N is always located at right bottom of the image, $|\overline{ON}|$ is the pixel distance between the point N and the image coordinate origin O . The constant T is the length (m) of the diagonal line in the rectangle area that consists of 4×7 squares.

Real fishes have a number of verebras that act as many mini-joints, thus their bodies move smooth during swimming. However, our Crangiform robotic fish only have five links. Based on the multi-joint robotic model, eight points are chosen in each sequence image to estimate the state of the fish actuation parts. According to the model shown in Fig.1, the state values of the fish actuators $\phi_i(t)$ at time t can be calculated by using basic geometric methods. For example, the angle $\phi_1(t)$ between link AB and link BC can be described as:

$$\phi_1(t) = \arctan((k_{BC}(t) - k_{AB}(t))/(1 + k_{AB}(t) \cdot k_{BC}(t)))$$

where $k_{AB}(t)$ or $k_{BC}(t)$ is the slope of the link calculated according to two points AB or BC at time t .

B. Three basic Carangiform swimming patterns

In our research, three basic Carangiform swimming patterns that primarily generated by the tail movement are abstracted. They are “cruise”, “cruise in turning” and “C sharp turning”. These three swimming patterns are most common basic Carangiform swimming patterns.

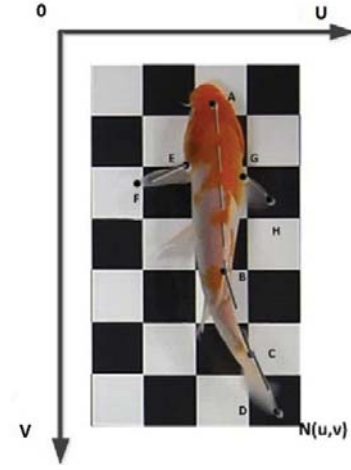


Fig. 5. The carp swimming image, eight features points are selected for estimating the joint angles. Point A is the center point between two eyes of the fish. The length of the straight line between point B and point C is one-third of the length of the fish body. Points C and D are located on the penduncle and the tail end. Points E, F, G and H are distributed on the top and end of the two pectoral fins.

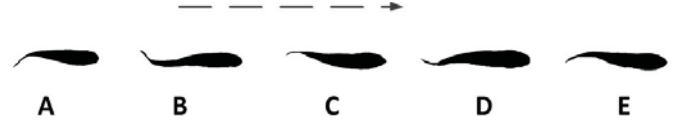


Fig. 6. “Cruise” swimming pattern profile extracted from images.

1) “cruise” swimming pattern: As shown in Fig.6, in “cruise” swimming pattern, the fish continues to move in a nearly straight line at a more or less constant speed. The fish body segments and the tail flap periodically, while the pectoral fins extend to help keep body balance.

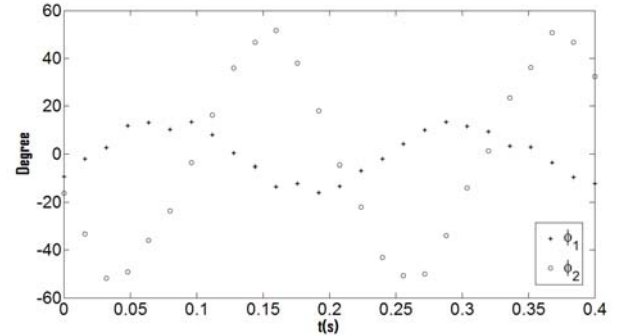


Fig. 7. Trajectories of joint angles (ϕ_1 and ϕ_2) in “cruise” swimming pattern extracted from the carp swimming observations.

Fig.7 shows the trajectories of joint angles ϕ_1 and ϕ_2 in “cruise” swimming patterns. According to empirical observations, the movements of the two joint angles in “cruise” swimming pattern can be formulated as two sinusoid functions. Moreover, as pointed out in [6], the motion of fish body during cruise can be described by a traveling wave. Thus, the two sinusoid functions have identical period but different phase,

they are described as:

$$\begin{aligned}\phi_1(t) &= A_1 \sin \omega t \\ \phi_2(t) &= A_2 \sin(\omega t + \theta)\end{aligned}$$

where, ω is the frequency of $\phi_1(t)$ and $\phi_2(t)$, A_1 and A_2 are the amplitudes, θ is the phase-difference between $\phi_1(t)$ and $\phi_2(t)$. Fig.8 shows the prototype of joint angles movements in “cruise” swimming pattern.

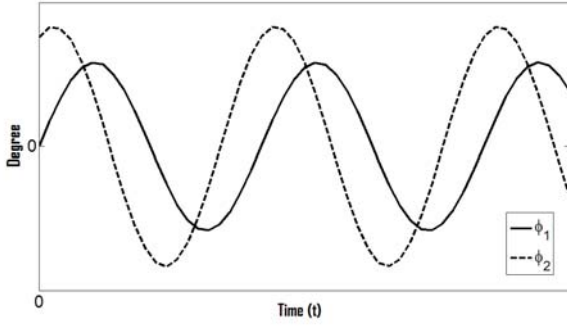


Fig. 8. Prototype of joint angles movements in “cruise” swimming pattern.

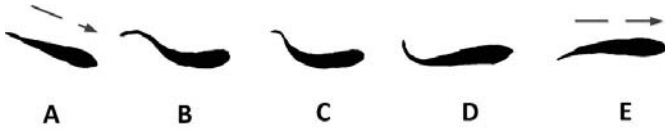


Fig. 9. “Cruise in turning” swimming pattern profile extracted from images.

2) “cruise in turning” swimming pattern: As shown in Fig.9, in “cruise in turning” swimming pattern, the fish turns with a low angular speed and at a constant linear speed. The pectoral fins sometimes assist body in turning, but most times assist body balance.

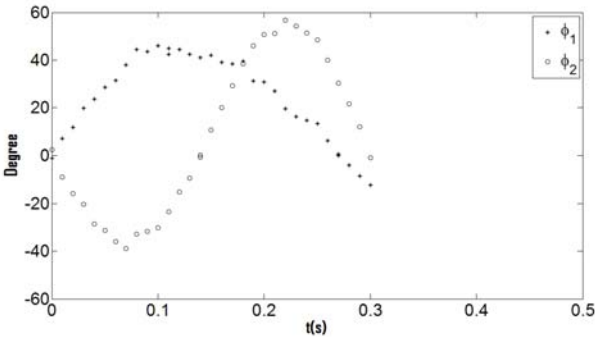


Fig. 10. Trajectories of joint angles (ϕ_1 and ϕ_2) in “Cruise in turning” swimming pattern extracted from the carp swimming observations.

Fig.10 shows the trajectories of joint angles ϕ_1 and ϕ_2 in “cruise in turning” swimming patterns. According to empirical observations, in a “cruise in turning” period, the movements of joint angles can be formulated as two functions composed

by a number of sinusoid. As shown in Fig.11, $\phi_1(t)$ and $\phi_2(t)$ are described as:

$$\begin{aligned}\phi_1(t) &= \mp \begin{cases} A_1^s \sin(\frac{\pi}{2t_1^s} t), & t \leq t_1^s, \\ A_1^s \sin[\frac{\pi}{2(T^s - t_1^s)}(t + T^s - 2t_1^s)], & t > t_1^s. \end{cases} \\ \phi_2(t) &= \pm \begin{cases} A_2^s \sin(\frac{\pi}{t_2^s} t), & t \leq t_2^s, \\ A_2^s \sin[\frac{\pi}{(T^s - t_2^s)}(t + T^s - 2t_2^s)], & t > t_2^s. \end{cases}\end{aligned}$$

where T^s is the period of turning, A_1^s , A_2^s , and $A_2'^s$ are the amplitudes, t_1^s and t_2^s are the switch point between different sinusoid functions. Positive and negative signs indicate the direction of fishes turning.

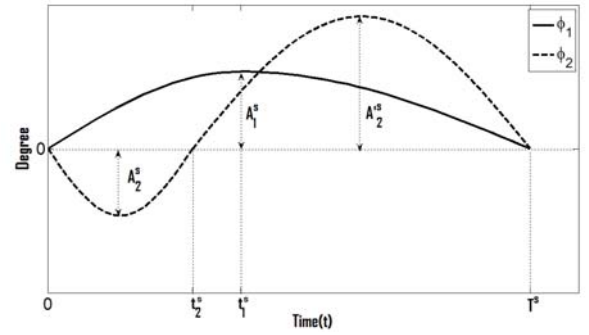


Fig. 11. Prototype of joint angles movements in “cruise in turning” swimming pattern. T^s is the period of turning, A_1^s, A_2^s , and $A_2'^s$ are the amplitudes, t_1^s and t_2^s are the switch point between different sinusoid functions.

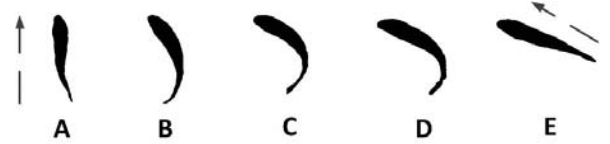


Fig. 12. “C sharp turning” swimming pattern profile extracted from images.

3) “C sharp turning” swimming pattern: “C sharp turning” is a special fish maneuvering motion. As shown in Fig.12, the fish bends its rear body quickly in a C-shape to change its swimming direction in a very small space.

Fig.13 shows the trajectories of joint angles ϕ_1 and ϕ_1 in “C sharp turning” swimming patterns. According to empirical observations, shown as in Fig.14, the movements of joint angles ϕ_i ($i = 1, 2$) in “C sharp turn” can be modeled as follows:

$$\phi_i(t) = \pm \begin{cases} A_i^c [1 + \sin(\frac{\pi}{2t_i^c} t - \frac{\pi}{2})], & t \leq t_i^c, \\ A_i^c \sin[\frac{\pi}{2(T^c - t_i^c)}(t + T^c - 2t_i^c)], & t > t_i^c. \end{cases}$$

where T^c is the period of turning, A_i^c are the amplitudes, t_i are the switch points between different sinusoid functions. Positive and negative signs indicate the direction of fishes turning.

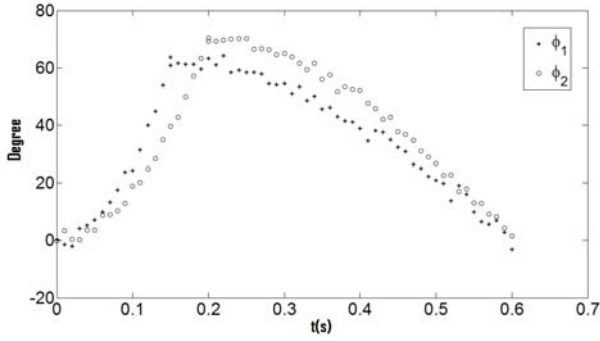


Fig. 13. Trajectories of joint angles (ϕ_1 and ϕ_2) in “C sharp turning” swimming pattern.

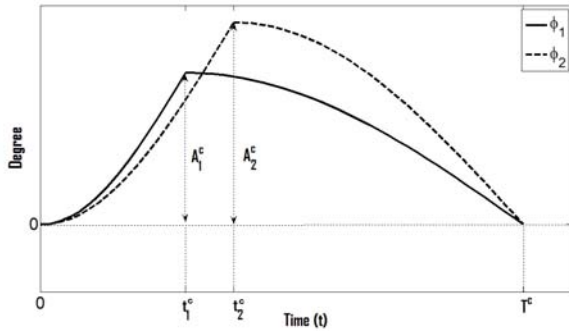


Fig. 14. Prototype of joint angles movements in “C sharp turning” swimming pattern. T^c is the period of turning, A_i^c are the amplitudes, t_i are the switch points between different sinusoid functions.

C. Similar swimming pattern regeneration

Note that real fishes and robotic fishes are different in various aspects such as size, structure, volume, surface, and actuation. We need to tune the real fish swimming patterns so as to fit robotic fish locomotion. Based on the swimming pattern prototypes, similar swimming patterns can be easily regenerated through tuning the parameters of swimming pattern prototypes. However, these parameters cannot be given arbitrary. Since the movements of the different actuation joints are coordinated when fishes swim, and it is difficult to model these coordinate relations explicitly. Typically, the setting of these parameters should generate a body wave according to fish swimming character. In other words, if the kinematic model of fish in a special swimming pattern could be obtained, the parameters of similar swimming patterns could be determined through some body wave fitting approaches (eg. [3] and [7]). Unfortunately, most kinematic models that generate fish swimming patterns are still unknown. Moreover, as pointed from [8], the current body wave fitting approaches have high computational complexity.

In this work, the similar swimming patterns are easily regenerated since the swimming pattern models described in this paper are composed by a number of sinusoid functions. Firstly, the parameters are given according to real fish swimming observations. Then, the original pattern according to observations

can be easily stretched and compressed along the temporal coordinate and spatial coordinates by tuning the amplitudes, frequency and phase of the sinusoid functions. For example, in “cruise in turning” swimming pattern, Fig.15(a) shows the joint movement trajectories generated by pattern model whose parameters are obtained according to observations (see Fig.7). Fig.15(b) shows the similar pattern regenerated by turning parameters.

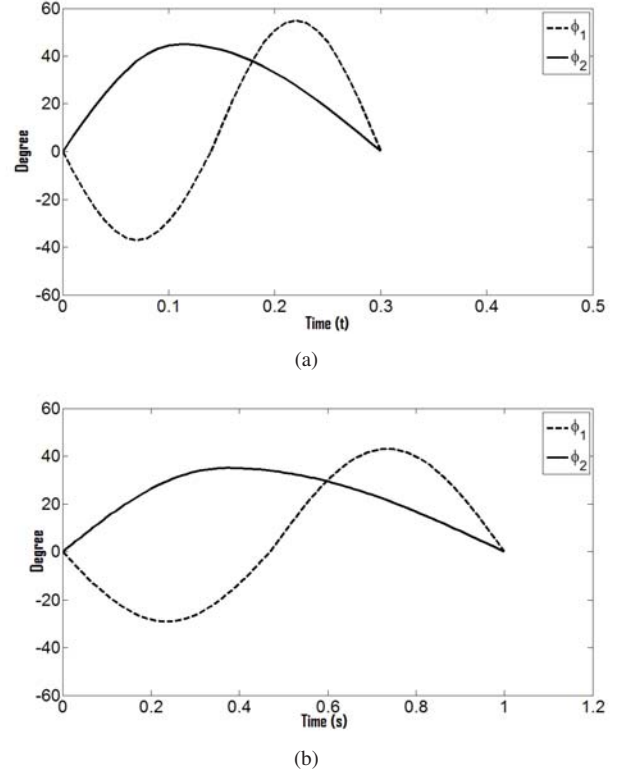


Fig. 15. Joint movement trajectories generated by “cruise in turning” swimming pattern model. (a) Parameters obtained base on observations, $T^s = 0.3$, $t_1^s = 0.11$, $t_2^s = 0.14$, $A_1^s = 45$, $A_2^s = 37$, and $A_2'^s = 55$. (b) Similar pattern generated by turning parameters, $T^s = 1$, $t_1^s = 0.37$, $t_2^s = 0.47$, $A_1^s = 35$, $A_2^s = 29$, and $A_2'^s = 43$

IV. EXPERIMENTS AND RESULTS

To illustrate the feasibility and effectiveness of the proposed approach, three basic swimming patterns are applied to carry out the robotic fish described in Section II. The experiments are in a swimming tank with size of 300cm \times 180cm and with still water of 500mm in depth.

A. cruise straight experiment

According to the model of joint angel movements in “cruise” swimming pattern, there are four parameters to be tuned, namely, A_1 , A_2 , ω , and θ . Imitating the carp swimming we observed, set $A_1 = 45$, $A_2 = 60$, $\theta = 3.5$. Because of limited actuation points, the robotic fish cannot move as fast as the carp, thus we set $\omega = 6.28$ to make the period of the joint movements extended from 0.3 seconds to one seconds.

Fig.16 shows the robotic fish swimming in “cruise” swimming pattern.

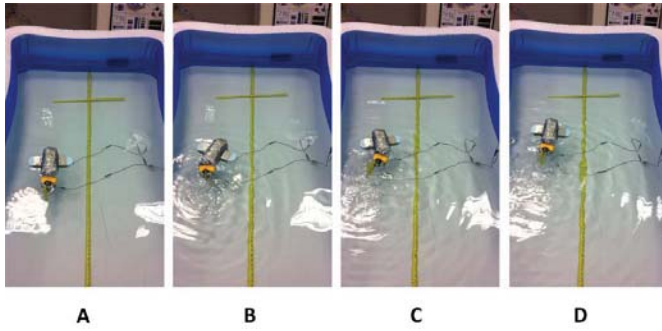


Fig. 16. The robotic fish is swimming in “cruise” swimming pattern.

B. “cruise in turning” experiment

To cater to the actual platform, a similar “cruise in turning” swimming pattern is generated by turning parameters: $T^s = 1$, $t_1^s = 0.37$, $t_2^s = 0.47$, $A_1^s = 35$, $A_2^s = 29$, and $A_2^s = 43$. Comparing with the original pattern abstracted from the carp swimming (see Fig.13), the new similar pattern is stretched along the temporal coordinate and compressed along the spatial coordinate in proportion (see Fig.15). In this experiment, the “cruise in turning” is completed within one seconds. Fig.17 shows the robotic fish swimming in “cruise in turning” swimming pattern.

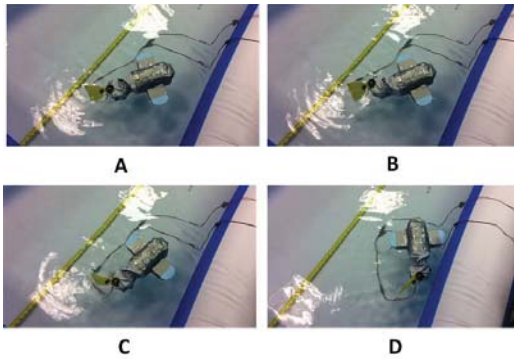


Fig. 17. The robotic fish is swimming in “cruise in turning” swimming pattern.

C. “C sharp turning” experiment

According to the model of joint angels movement in “C sharp turning” swimming pattern, there are five parameters to be tuned, namely, A_1^c , A_2^c , t_1^c , t_2^c , and T^c . In this experiment, we intend to make the robotic fish turn anticlockwise within one second, thus we set $A_1^c = 55$, $A_2^c = 65$, $t_1^c = 0.25$, $t_2^c = 0.35$, and $T^c = 1$. Fig.18 shows the robotic fish swimming in “C sharp turning” swimming pattern.

V. CONCLUSION

This paper focus on making a multi-joint robotic fish to realize Carangiform swimming patterns through observations

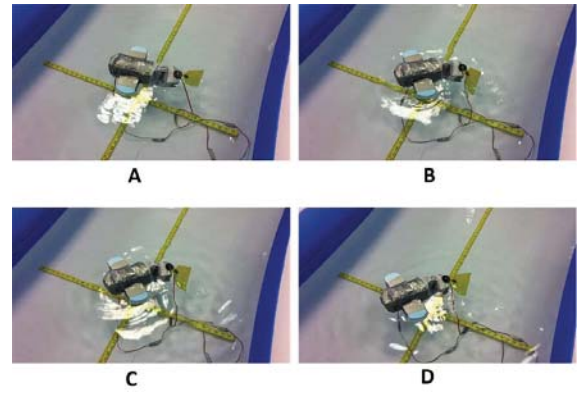


Fig. 18. The robotic fish is swimming in “C sharp turning” swimming pattern.

of real fish swimming. According to observations on a real carp swimming, three basic swimming patterns are abstracted and modeled from robotic perspective. Base on these models, various similar motion patterns are regenerated by tuning parameters to cater to actual robot platform. Finally, these patterns are implemented on a multi-joint robotic fish, and the experiment results show the feasibility of the approach.

REFERENCES

- [1] M.Sfakiotakis, D.M.Lane, and J. Davies, “Reviw of fish swimming modes for aquatic locomotion,” *IEEE Journal of Oceanic Engineering*, vol. 24, no. 2, pp. 237 – 252, 1999.
- [2] J. Colgate and K. M.Lynch, “Mechanics and control of swimming: a review,” *IEEE Journal of Oceanic Engineering*, vol. 29, no. 3, pp. 660 – 673, 2004.
- [3] J. Liu and H. Hu, “Biological inspiration: from carangiform fish to multi-joint robotic fish,” *Journal of bionic engineering*, vol. 7, no. 1, pp. 35 – 48, 2010.
- [4] S. D. Kelly and R. M. Murray, “Modelling efficient pisciform swimming for control,” *International Journal of Robust and Nonlinear Control*, vol. 10, pp. 217–241, 2000.
- [5] S. D. Kelly, R. J. Mason, C. T. Anhalt, R. M. Murray, and J. W. Burdick, “Modelling and experimental investigation of carangiform locomotion for control,” in *Proceedings of the American Control Conference*, vol. 1, 1998, pp. 1271–1276.
- [6] L. M. J., “Note on the swimming of slender fish,” *Journal of fluid mechanics*, vol. 9, no. 1, pp. 305–317, 1960.
- [7] J. Liu and H. Hu, “Mimicry of sharp turning behaviours in a robotic fish,” in *Internation conference on robotic and automation*, vol. 1, 2005, pp. 3329–3334.
- [8] W.Zhao, Y.Hu, and L.Wang, “Design and cpg - based control of biomimetic robotic fish,” *IET control theory and applications*, vol. 3, pp. 281–293, 2009.
- [9] A.J.Ijspeert, “A connectionist central pattern generator for the aquatic and terrestrial gaits of a simulated salamander,” *Biological Cybernetics*, vol. 84, no. 1, pp. 331–348, 2001.